

# Investigating Structural Changes in the Lipid Bilayer upon Insertion of the Transmembrane Domain of the Membrane-Bound Protein Phospholamban Utilizing $^{31}\text{P}$ and $^2\text{H}$ Solid-State NMR Spectroscopy

Paresh C. Dave, Elvis K. Tiburu, Krishnan Damodaran, and Gary A. Lorigan

Department of Chemistry and Biochemistry, Miami University, Oxford, Ohio

**ABSTRACT** Phospholamban (PLB) is a 52-amino acid integral membrane protein that regulates the flow of  $\text{Ca}^{2+}$  ions in cardiac muscle cells. In the present study, the transmembrane domain of PLB (24–52) was incorporated into phospholipid bilayers prepared from 1-palmitoyl-2-oleoyl-*sn*-glycero-phosphocholine (POPC). Solid-state  $^{31}\text{P}$  and  $^2\text{H}$  NMR experiments were carried out to study the behavior of POPC bilayers in the presence of the hydrophobic peptide PLB at temperatures ranging from 30°C to 60°C. The PLB peptide concentration varied from 0 mol % to 6 mol % with respect to POPC. Solid-state  $^{31}\text{P}$  NMR spectroscopy is a valuable technique to study the different phases formed by phospholipid membranes.  $^{31}\text{P}$  NMR results suggest that the transmembrane protein phospholamban is incorporated successfully into the bilayer and the effects are observed in the lipid lamellar phase. Simulations of the  $^{31}\text{P}$  NMR spectra were carried out to reveal the formation of different vesicle sizes upon PLB insertion. The bilayer vesicles fragmented into smaller sizes by increasing the concentration of PLB with respect to POPC. Finally, molecular order parameters ( $S_{\text{CD}}$ ) were calculated by performing  $^2\text{H}$  solid-state NMR studies on deuterated POPC (*sn*-1 chain) phospholipid bilayers when the PLB peptide was inserted into the membrane.

## INTRODUCTION

Methods for understanding interactions between proteins and lipids are essential for elucidating biological structure-function relationships. Peptide-lipid interactions can affect both protein and bilayer structure (Bloom et al., 1991; Lemmon and Engelman, 1994a; Watts, 1993). Previous studies have suggested that these interactions can serve several regulatory roles such as controlling the membrane-association of lytic peptides, modulating membrane-protein activity, promoting peptide aggregation, segregating proteins within the membrane, determining protein sorting during secretion recognition (Arora and Tamm, 2001; Dempsey et al., 1986; Lemmon and Engelman, 1994b; Watts, 1981). Three typical models of biological membranes are planar lipid bilayers, vesicles (liposomes) and monolayers. According to Singer-Nicholson's model of a cell membrane, a lipid bilayer resembles a biomembrane closer than a monolayer (Singer and Nicolson, 1972). Liposomes or phospholipid dispersions are commonly used to study membrane structure upon peptide insertion (Epand, 1998; Liu et al., 2001). In an aqueous solution, phospholipids self-assemble to form lipid bilayers rather than micelles. The reason is that phosphatidylcholines have two acyl chains that are more or less parallel to one another. The overall shape of a phospholipid molecule is approximately rectangular, so these molecules are too bulky to fit in the interior of micelles. The well-defined synthetic membranes

are used as model systems to mimic the properties of biological membranes. Interestingly, the lipid bilayer in biological membranes is generally in the liquid-crystalline phase where the axis of symmetry of the acyl chain motion is perpendicular to the plane formed by the polar head-group.

High-resolution NMR techniques are now routinely employed to study the structure of complex macromolecules in solution (Brunner et al., 2000; Cavagnero et al., 1999; Ottiger and Bax, 1999; Vold et al., 1997). An alternative approach to solution structural studies of membrane macromolecules is the determination of their structural and dynamic properties using solid-state NMR spectroscopy. Solid-state NMR spectroscopy has been widely used to study the structure and dynamics of peptides, including those that associate with membranes or with biomineral surfaces (Barre et al., 2003; Cross, 1997; Long et al., 1998, 2001; Marassi et al., 1999; Marassi and Opella, 1998; Marcotte et al., 2003; Nakazawa and Asakura, 2003; Nicholson and Cross, 1989; Shaw et al., 2000; Watts, 1998). For membrane-bound peptides, solid-state NMR spectroscopy has the ability to probe lipid bilayers in the presence of a peptide, which can be poised in a biologically relevant liquid-crystalline state. Membrane proteins reconstituted into synthetic phospholipid bilayers simulate the biological membrane better than detergent micelles such as sodium dodecyl sulfate (Morrow and Grant, 2000; Rigby et al., 1996; Sharpe et al., 2002a,b).

Phospholamban (PLB) is a small transmembrane peptide (52 amino acids) that interacts with the  $\text{Ca}^{2+}$ -ATPase pump and lowers its affinity for  $\text{Ca}^{2+}$  (Simmerman et al., 1986, 1996; Simmerman and Jones, 1998; Stokes, 1997; Yao et al., 2001). It consists of three domains: residues 1–20 (hydrophilic cytoplasmic domain), residues 21–30 (hinge segment),

Submitted September 8, 2003, and accepted for publication November 4, 2003.

Address reprint requests to Gary A. Lorigan, Dept. of Chemistry and Biochemistry, Miami University, Oxford, OH 45056. Tel.: 513-529-4703; Fax: 513-529-5715; E-mail: lorigag@muohio.edu.

© 2004 by the Biophysical Society

0006-3495/04/03/1564/10 \$2.00

and residues 31–52 (hydrophobic  $\alpha$ -helical membrane-spanning region). Because of its biological importance and its relatively small size, PLB has been the benchmark used in many theoretical and experimental studies of membrane protein structure and assemblies. Fujii and co-workers elucidated the complete PLB primary structure by amino acid sequencing (Fujii et al., 1987). They established that the molecular mass of the PLB monomer was 6082 Da and determined that PLB is a pentamer consisting of five identical subunits.

Determining the structure of PLB and its interactions with the lipid bilayer is central for understanding its regulatory role (Mascioni et al., 2002a,b; Ying et al., 2000). The transmembrane segment of PLB (24–52) has been synthesized using solid-phase peptide synthesis and purified according to the modified method reported recently by our group (Tiburu et al., 2003). In the present study, the transmembrane domain of PLB (24–52) was incorporated into phospholipid bilayers prepared from 1-palmitoyl-2-oleoyl-*sn*-glycero-phosphatidylcholine (POPC). Solid-state NMR spectroscopy has been used to monitor the interactions between the lipid bilayers and PLB, by exploiting the  $^{31}\text{P}$  nuclei as a natural spin reporter on the headgroup of POPC. Solid-state  $^{31}\text{P}$  NMR spectroscopy is a valuable technique to study the different phases formed by model phospholipid membranes (Cullis and de Kruijff, 1979; Seelig, 1978). The  $^{31}\text{P}$  NMR line shapes have distinct characteristics for different lipid phases such as the gel and liquid crystalline lamellar phases, the inverted hexagonal phase, and isotropic phases such as small vesicles or micelles (Smith and Ekiel, 1984). The low chain melting point of POPC makes it possible to examine PLB in membranes at a physiologically relevant temperature utilizing solid-state NMR spectroscopy. In the present paper, we are focusing on three main points: 1), lipid-peptide interactions of PLB incorporated into POPC bilayers utilizing  $^{31}\text{P}$  NMR spectroscopy; 2), perturbations of the phospholipid bilayers using POPC- $\text{d}_{31}$  as a NMR probe; and 3), the effects of various concentrations of PLB and temperature on the dynamic properties of the phospholipid bilayers.

## MATERIALS AND METHODS

### Materials

9-Fluorenylmethoxycarbonyl (Fmoc)-amino acids and other chemicals for peptide synthesis were purchased from Applied Biosystems (Foster City, CA). POPC and POPC- $\text{d}_{31}$  were purchased from Avanti Polar Lipids (Alabaster, AL). Prior to use, phospholipids were dissolved in chloroform and stored at  $-20^\circ\text{C}$ . Chloroform, hexafluoro-2-propanol, formic acid, and 2,2,2-trifluoroethanol (TFE) were purchased from Sigma-Aldrich (Milwaukee, WI). High performance liquid chromatography-grade acetonitrile and 2-propanol were obtained from Pharmco (Brookfield, CT) and were filtered through a 0.22- $\mu\text{m}$  nylon membrane before use. Water was purified using a Nanopure reverse osmosis system (Millipore, Bedford, MA). N-[2-hydroxyethyl]piperazine-N'-2-ethane sulfonic acid (HEPES) and EDTA were obtained from Sigma-Aldrich.

### Synthesis and purification of PLB

PLB was synthesized according to the recently published procedure (Tiburu et al., 2003). In brief, PLB was synthesized using modified Fmoc-based solid-phase methods with an ABI 433A peptide synthesizer (Applied Biosystems, Foster City, CA). The sequence of the synthesized transmembrane segment of PLB (24–52) is ARQNLQNLFNFCILICLLLCIIIVMLL. The crude peptide was purified on an Amersham Pharmacia Biotech AKTA explorer 10S high performance liquid chromatograph controlled by Unicorn (version 3) system software. A  $\text{C}_4$  semipreparative polymer supported column (259VHP82215) was acquired from Grace Vydac (Hesperia, CA). Columns were equilibrated with 95% solvent A and 5% solvent B. Solvent A consisted of  $\text{H}_2\text{O}$  and solvent B was 38% MeCN, 57% IPA, and 5%  $\text{H}_2\text{O}$ . Elution of the peptide was achieved with a linear gradient to a final solvent composition of 93% solvent B. The purified peptide was lyophilized and characterized by matrix-assisted laser desorption ionization time-of-flight mass spectrometry.

### NMR sample preparation

The POPC-rich bilayer samples, containing various mol % of peptide to phospholipid, were prepared following a slightly modified protocol given by Rigby and co-workers. (1996). POPC (76 mg) and PLB were dissolved in  $\text{CHCl}_3$  and TFE, respectively, and added to a  $12 \times 75$ -mm test tube. The solvents were removed under a steady stream of  $\text{N}_2$  gas for  $\sim 15$ –20 min. The test tube was placed in a vacuum desiccator overnight to remove any residual solvents. The peptide/lipid mixture was resuspended in 190  $\mu\text{L}$  HEPES buffer (5 mM EDTA, 20 mM NaCl, and 30 mM HEPES, pH 7.0) by heating in a water bath at  $50^\circ\text{C}$  along with slight frequent sample agitation to avoid frothing the mixture. After all the phospholipids were fully dissolved, the sample was transferred to a NMR sample tube. POPC- $\text{d}_{31}$  (4 mg) was added to the samples when conducting the  $^2\text{H}$  NMR experiments.

### NMR spectroscopy

$^{31}\text{P}$  NMR spectra were recorded on a Bruker Avance 500-MHz solid-state NMR spectrometer operating at 202.4 MHz using a Bruker double resonance 5-mm round coil static probe (Bruker, Billerica, MA). The  $^{31}\text{P}$  NMR spectra were recorded with  $^1\text{H}$  decoupling using a  $4\text{-}\mu\text{s}$   $\pi/2$  pulse for  $^{31}\text{P}$  and a 5-s recycle delay. For the  $^{31}\text{P}$  NMR spectra 1024 scans were taken and the free induction decay was processed using 100 Hz of line broadening. The spectral width was set to 150 ppm.  $^2\text{H}$  NMR spectra were recorded on the same NMR spectrometer operating at 76.77 MHz using the same 5-mm static round coil NMR probe. The quadrupolar echo pulse sequence was employed using quadrature detection with complete phase cycling of the pulse pairs (Davis et al., 1976). The  $90^\circ$  pulse length was 3  $\mu\text{s}$ , the interpulse delay was 20  $\mu\text{s}$ , the recycle delay was 0.4 s, and the spectral width was set to 100 kHz. A total of 12,288 transients was averaged for each spectrum and processed using 200 Hz line broadening. The sample was held at the desired temperature for 10 min prior to signal acquisition.

### NMR data analysis

Simulation of  $^{31}\text{P}$  NMR spectra was carried out using the software program called DMFIT (Massiot et al., 2002). This program permits the fitting or modeling of experimental 1D and 2D spectra to a sum of lines or contributions characterized by their corresponding NMR parameters. The spectral fittings were conducted using a minimum number of species. Static chemical shift anisotropy spectral patterns were considered for all the species. Lorentzian broadening was used for all simulations.

Powder-type  $^2\text{H}$  NMR spectra of multilamellar dispersions of POPC- $\text{d}_{31}$  were numerically deconvoluted (dePaked) using the algorithm of McCabe and Wassall (1995, 1997). The spectra were deconvoluted such that the bilayer normal was perpendicular with respect to the direction of the static

magnetic field. The quadrupolar splittings were directly measured from the dePaked spectra and converted into order parameters according to the following expression (Dave et al., 2003; Huster et al., 2002):

$$\Delta\nu_Q^i = 3/4(e^2qQ/h)S_{CD}^i$$

where  $\Delta\nu_Q^i$  is the quadrupolar splitting for a deuteron attached to the  $i$ th carbon,  $e^2qQ/h$  is the quadrupolar splitting constant (168 kHz for deuterons in C- $^2$ H bonds), and  $S_{CD}^i$  is the chain order parameter for a deuteron attached to the  $i$ th carbon of the acyl chain of POPC. The  $^2$ H nuclei attached to the terminal methyl carbons were assigned carbon number 15. The remaining  $^2$ H assignments were made in decreasing order along the phospholipid acyl chain. Thus, the corresponding order parameters for the individual C-D methylene groups and the terminal methyl groups of the acyl chains were directly evaluated from the quadrupole splittings of the dePaked  $^2$ H NMR spectra. The  $^2$ H peaks in the NMR spectra were assigned based upon the dynamic properties of the individual CD $_3$  and CD $_2$  groups. The quadrupole splittings of the CD $_3$  methyl groups at the end of the acyl chains are the smallest and closest to 0 kHz because they rotate at the fastest frequency. The next smallest splitting was assigned to the  $^2$ H attached to C-14 and so forth along the acyl chain. The quadrupole splittings for the deuterons in the plateau region were estimated by integration of the last broad peak according to the literature (Huster et al., 1998). The order parameters calculated for the CD $_3$  quadrupole splitting were multiplied by 3 according to the literature (Dufourc et al., 1984; Stockson et al., 1976).

## RESULTS AND DISCUSSION

### $^{31}\text{P}$ NMR study of PLB incorporated into POPC bilayer

$^{31}\text{P}$  NMR spectroscopic measurements were performed to determine the nature of the various lamellar and nonlamellar phase transitions exhibited by the transmembrane segment of PLB incorporated into POPC phospholipid bilayers. The static  $^{31}\text{P}$  NMR spectra of the POPC phospholipid bilayer with and without 1 mol % of the hydrophobic segment of PLB are shown in Fig. 1, *A* and *B*, respectively. The  $^{31}\text{P}$  powder-pattern NMR spectra were recorded at temperatures ranging from 30°C to 60°C. The motionally averaged powder-pattern spectra are characteristic of phospholipid bilayers in the liquid crystalline phase ( $L_\alpha$ ) and are expected for POPC at a temperature well above its chain melting transition temperature of  $-3^\circ\text{C}$  (Seelig, 1978). The spectra in the absence and in the presence of 1 mol % PLB showed a similar powder lineshape, both with  $\eta = 0$  (axial symmetry). The spectra indicate that the lipid bilayers remain in the  $L_\alpha$  phase even after addition of 1 mol % phospholamban with respect to POPC, and do not form

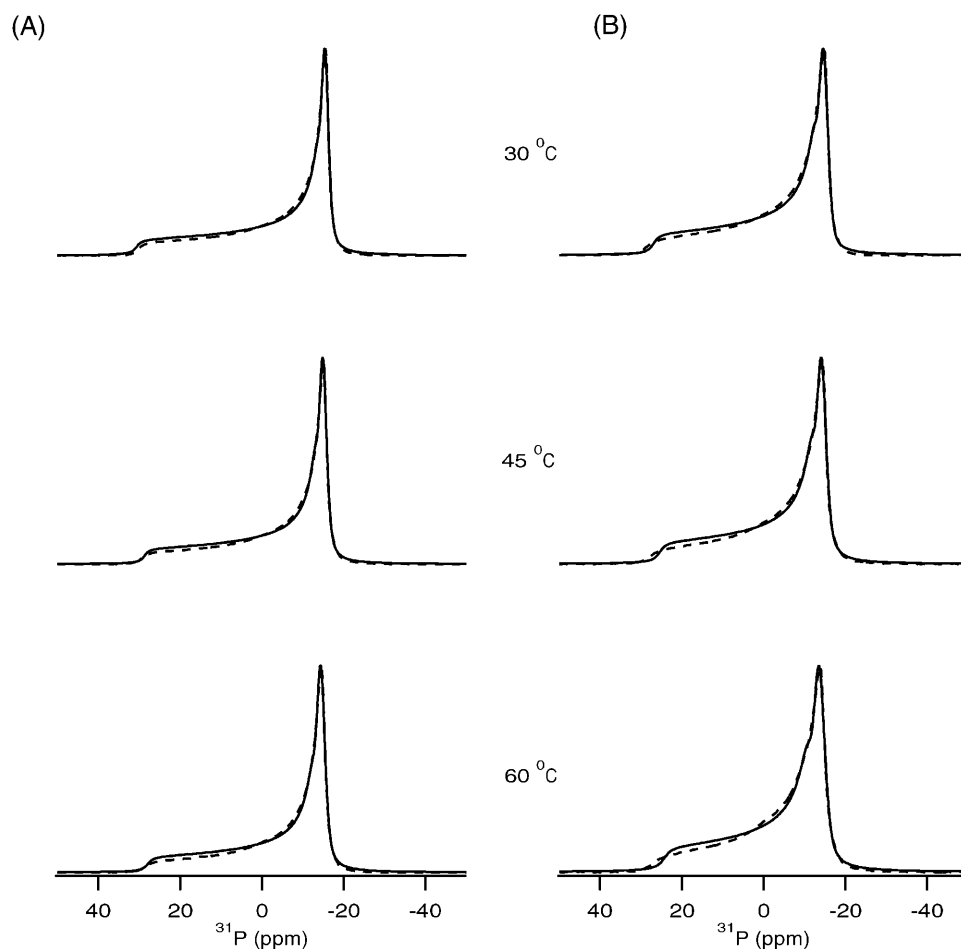


FIGURE 1  $^{31}\text{P}$  NMR spectra of POPC phospholipid bilayers investigated as a function of temperature. (*A*) In the absence of PLB, spectra are shown for pure POPC bilayers. (*B*)  $^{31}\text{P}$  spectra are shown for the POPC bilayer in the presence of 1 mol % PLB with respect to POPC. The solid-line spectra represent the experimental results and the dotted-line spectra represent best-fit simulated spectra corresponding to the experimental spectra.

isotropic or inverse hexagonal phases with high curvatures. In the  $L_\alpha$  phase, a POPC bilayer has been determined to have a hydrophobic thickness of  $\sim 27$  Å (Harzer and Bechinger, 2000; Nezil and Bloom, 1992). The entire thickness of the POPC phospholipid bilayer is  $\sim 50$ – $54$  Å (Huber et al., 2002). If the hydrophobic region of PLB (24–52) is 100%  $\alpha$ -helical then it would be  $\sim 43$  Å in length (Jones et al., 1994). This indicates that the POPC bilayer is a close match in thickness to the transmembrane segment of PLB and hydrophobic mismatch is not a serious problem under these conditions. The peptide is incorporated into the bilayer without distorting the lipid structure. Hydrophobic mismatch for model peptides KK(LA)<sub>15</sub>KK (45 Å hydrophobic length) have been studied in detail using  $^{31}\text{P}$  and  $^{15}\text{N}$  NMR spectroscopy (Harzer and Bechinger, 2000). Those results clearly suggest that the POPC bilayer is a perfect match for hydrophobic peptides with a 36- to 45-Å length. A dioleoyl phosphatidyl choline (DOPC) bilayer has been used previously for incorporation of AFA-PLB into a mechanically oriented membrane system (Mascioni et al., 2002a). The  $^{31}\text{P}$  NMR spectra of POPC samples containing no PLB and with 1 mol % PLB were found to possess chemical shift anisotropy (CSA; in this paper, CSA is  $\sigma_{\parallel} - \sigma_{\perp}$ ) widths of

44 ppm and 41 ppm, respectively (Seelig, 1978; Sharpe et al., 2002a,b). A somewhat smaller ( $\sim 3$  ppm)  $^{31}\text{P}$  CSA width is detected for the membrane-bound sample in our study as seen from the lineshape simulations. Similarly, in both cases by increasing the sample temperature, the CSA width decreases, indicating that the molecular motion in the phospholipid bilayer increases with temperature.

Higher concentrations of PLB were also incorporated into POPC bilayers to probe the peptide-lipid interactions. Fig. 2, A and B, show the experimental and simulated  $^{31}\text{P}$  NMR spectra of POPC bilayer samples containing 4 mol % PLB with respect to phospholipid. Similarly, Fig. 3, A and B, represent the experimental and simulated  $^{31}\text{P}$  NMR spectra of POPC bilayer samples containing 6 mol % PLB with respect to phospholipid. The results clearly indicate that PLB interacts with the headgroups of the POPC bilayer. This study was performed at temperatures ranging from 30°C to 60°C. The unoriented multilamellar liposome samples containing 0–6 mol % peptide were all found to produce  $^{31}\text{P}$  NMR powder-pattern spectra representing POPC in the  $L_\alpha$  phase even at higher temperatures (60°C). The membrane remains in the lamellar phase upon binding of PLB even at the highest peptide concentration (6 mol %) studied. The

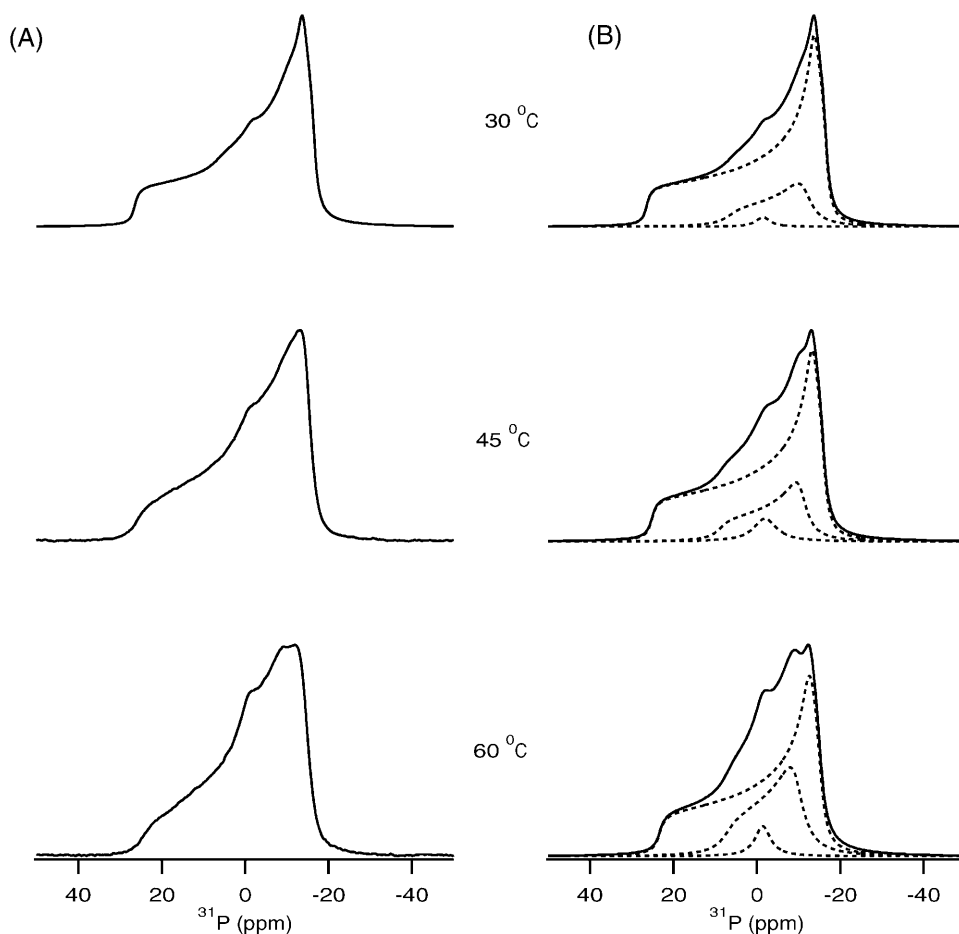


FIGURE 2  $^{31}\text{P}$  NMR spectra of POPC phospholipid bilayers in the presence of 4 mol % PLB with respect to POPC investigated as a function of temperature. (A) Experimental spectra. (B) The dotted-line spectra represent the simulated bilayer species having different vesicle sizes possessing different CSA widths. The solid-line spectra are the sum of the dotted-line spectra and represent the best-fit simulated spectra corresponding to the experimental spectra.

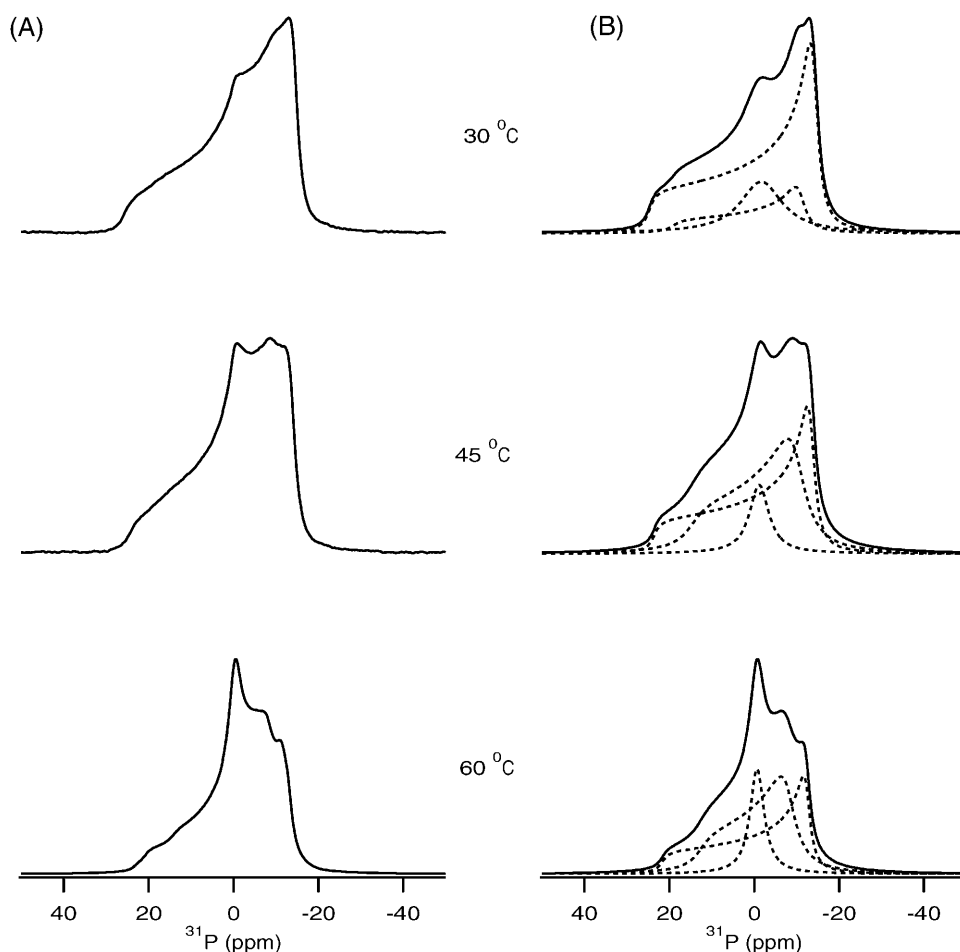


FIGURE 3  $^{31}\text{P}$  NMR spectra of POPC phospholipid bilayers in the presence of 6 mol % PLB with respect to the phospholipid POPC bilayers investigated as a function of temperature. (A) Experimental spectra. (B) The dotted-line spectra represent the simulated bilayer species having different vesicle sizes possessing different CSA widths. The solid-line spectra are the sum of the dotted-line spectra and represent the best-fit simulated spectra corresponding to the experimental spectra.

overall CSA spectral width is  $\sim 3$  ppm smaller when compared to the pure POPC membrane. This can be attributed to a faster rotation of the lipids when the membrane-associated PLB peptide partially disrupts the hydrogen bonding network between the lipid headgroups. At higher concentrations of PLB, the spectra represent superpositions of the different lamellar phases. Previously, the presence of two different anisotropic or lamellar phases was observed in the spectral simulations of  $^{31}\text{P}$  NMR spectra of cardiotoxin incorporated into 1,2-dimyristoyl-*sn*-glycero-3-phosphocholine bilayers (Auger, 1997). Also, Strandberg and co-workers reported the presence of three different lamellar phases upon incorporation of the peptide  $\text{KK(LA)}_8\text{KK}$  into DOPC bilayers utilizing  $^{31}\text{P}$  NMR spectroscopy (Strandberg et al., 2001). To fully understand the peptide-lipid interactions from  $^{31}\text{P}$  NMR, spectral simulations have been carried out as explained in the materials and method section (Figs. 2 B and 3 B). It is important to note here that the  $^{31}\text{P}$  chemical shift of phosphodiester, such as is found in membrane lipids, depends upon the molecular motions and orientation of the group with respect to the magnetic field of the spectrometer (Smith and Ekiel, 1984). The orientation of the headgroup depends upon the chem-

istry, hydration, hydrogen bonding, and charge interactions of each phospholipid headgroup.  $^{31}\text{P}$  NMR spectra are very sensitive to the rate of motions of lipids in the liquid crystalline phase, which usually have motional rates in the fast-limit region. Burnell and co-workers were able to simulate experimental spectra of DOPC vesicles of different sizes at various temperatures and viscosities of the medium (Burnell et al., 1980). The general results from these studies indicate that the spectral lineshape and CSA width are dependent upon the size of the vesicles. The CSA spectral width decreases with decreasing vesicle size, and isotropic lines are observed for very small vesicles. The formation of micelles or small vesicles by fragmentation of the bilayers and the observation of different phases has been observed previously on other membrane proteins utilizing  $^{31}\text{P}$  NMR spectra obtained from the phospholipids of mechanically oriented bilayers (Hori et al., 1999; Hallock et al., 2003; Henzler Wildman et al., 2003). The structural results gleaned from both aligned and unoriented solid-state NMR samples are important because the morphological membrane structure is different for the two methods.

The  $^{31}\text{P}$  NMR in Figs. 2 A and 3 A at higher concentrations of PLB clearly indicates that the presence of an isotropic

peak and a shallow high-field shoulder (near to  $\sigma_{\perp}$ ). The spectral simulations reveal the presence of different species of POPC bilayers (Figs. 2 B and 3 B). The interpretation of the  $^{31}\text{P}$  NMR spectra with the isotropic components is not certain (Pinheiro et al., 1997). In some studies, they have been attributed to vesicular or micellar structures on or within the bilayers, possibly associated with different phases (Cullis and de Kruijff, 1979; de Kruijff and Cullis, 1980). Others have attributed them to the presence of smaller diameter vesicles induced upon protein binding (Pinheiro and Watts, 1994a,b). Alternatively, the lineshapes may arise from a different  $^{31}\text{P}$  species, which undergoes molecular motion that yields isotropic chemical shift transitions. Despite the nonbilayer spectral component being broader from lipid-peptide complexes when compared to peptide-free bilayers, there is no indication of a well-defined hexagonal  $\text{H}_{\text{II}}$  phase. The spectral simulation of  $^{31}\text{P}$  NMR lineshape clearly indicates the presence of two different lamellar phases and one isotropic phase. The presence of two lamellar phases having different CSA width values also indicates the presence of multilamellar vesicles (MLVs) of different sizes forming different microdomains. The presence of an isotropic component indicates the existence of very small size vesicles like micelles. Interestingly, spectral simulations suggest the presence of different species at higher PLB concentrations, when compared to 1 mol % PLB in which case only one species is present (Fig. 1). The  $^{31}\text{P}$  NMR spectral lineshapes clearly indicate (Figs. 1–3) that the phospholipid bilayers are disrupted by increasing the concentration of PLB. The presence of one species having a similar large CSA width (41 ppm) was observed for the control and 1 mol % PLB sample and suggests the presence of large size MLVs. The smaller CSA width obtained for the other lamellar phases when 4% and 6 mol % PLB was added to the POPC bilayer suggests the presence of smaller size vesicles (Burnell et al., 1980). The large size vesicles can be fragmented to form microdomains composed of small size vesicles. The diameter of the vesicles can be calculated from the CSA width for different MLVs species (Burnell et al., 1980). At 1 mol % PLB with respect to POPC, larger MLVs with an approximate diameter of 25,000 Å are formed. When 4 mol % PLB was embedded into the bilayers two different size vesicles were formed with approximate diameters of 20,000 and 1500 Å. Additionally, the isotropic components suggest the presence of very small vesicles having diameters <1000 Å. Analysis of the 6 mol % PLB/POPC data indicates that large size vesicles fragmented and formed the components possessing vesicles with a diameter of ~10,000 and ~2500 Å, and one isotropic component with a diameter <1000 Å. The contributions of each component were calculated by integrating the area of the individual species and comparing it with the entire CSA width of the experimental spectrum. These results indicate that when 4 mol % PLB was incorporated into POPC, contributions from component I (large CSA width), component II (small CSA

width), and component III (isotropic species) are ~82%, ~17%, and ~1%, respectively, at 30°C. In addition to that, contributions from component I decreased from 82% to 67% and contributions from component II and component III increased from 17% to 26% and 1% to 7%, respectively, when the temperature was increased from 30°C to 60°C. Interestingly, at 30°C the sample containing 6 mol % PLB/POPC was found to have contributions from component I, component II, and component III of ~67%, ~25%, and ~8%, respectively. Contributions from component I decreased from 67% to 39% and increased for component II from 25% to 44% and for component III from 8% to 17% by increasing the temperature from 30°C to 60°C. A comparison of Figs. 2 and 3 indicates that the contribution from the anisotropic phases having smaller CSA widths increases as more PLB is incorporated into the phospholipid bilayers. One can see clearly from Figs. 2 and 3 that upon increasing the temperature the contributions from the different species change. At higher temperatures, molecular motions increase and small vesicles rotate faster. Also, lateral diffusion influences the  $^{31}\text{P}$  NMR lineshape of phospholipid bilayer (Burnell et al., 1980; Cullis and de Kruijff, 1979; Smith and Ekiel, 1984). Another possibility is that by increasing the amount of PLB incorporated into the POPC bilayer, the lateral diffusion rate of the lipids at higher temperature increases, resulting in a decrease in the CSA width of the  $^{31}\text{P}$  NMR spectra.

## **$^2\text{H}$ NMR study of PLB incorporated into POPC bilayer**

The effect of PLB on the order and dynamics of the acyl chains of the POPC bilayer have been studied using POPC- $\text{d}_{31}$  (deuterated palmitoyl acyl chain). The  $^2\text{H}$  NMR spectra of a dispersion of POPC- $\text{d}_{31}$  in the absence and in the presence of PLB at 35°C are shown in Fig. 4. Several conclusions can be immediately drawn from the  $^2\text{H}$  NMR lineshapes in Fig. 4. First, the spectra are characteristic of axially symmetric motions of the phospholipids about the bilayer normal and the spectra consist mostly of overlapping doublet resonances that result from the different  $\text{CD}_2$  segments of the acyl chain. The central doublet corresponds to the terminal  $\text{CD}_3$  group. Secondly, the spectral width is a measure of the fluidity of the lipid bilayer. The range observed in the POPC/POPC- $\text{d}_{31}$  is typical for acyl chains in a liquid-crystalline bilayer (Lafleur et al., 1989; Seelig and Seelig, 1974; Seelig and Niederberger, 1974). In Fig. 4, the spectral width of POPC- $\text{d}_{31}$  marginally decreases by increasing the PLB concentrations when compared to the control spectrum of pure POPC/POPC- $\text{d}_{31}$ . The marginal decrease in the spectral width suggests that the presence of the PLB peptide disorders the acyl chains to some extent for all the different PLB/POPC concentrations. It also reveals that the POPC bilayer is still in the liquid-crystalline  $\text{L}_{\alpha}$  phase. This supports our  $^{31}\text{P}$  NMR results as discussed

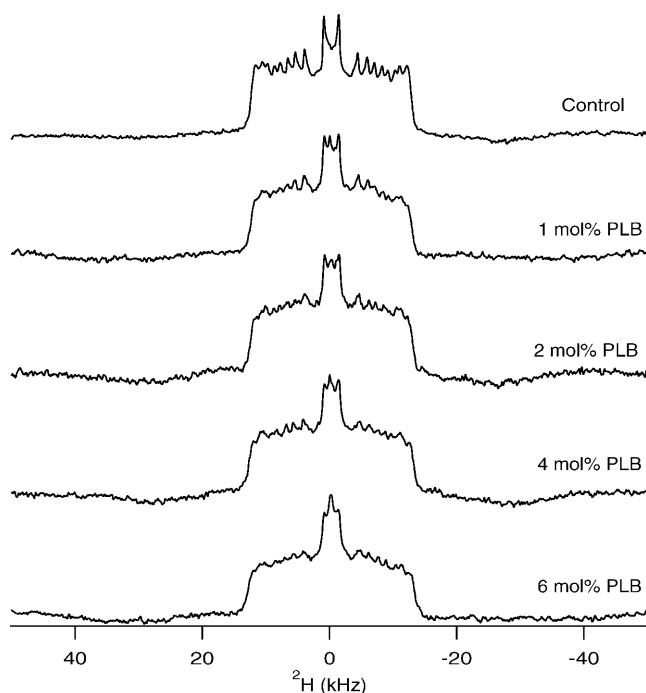


FIGURE 4  $^2\text{H}$  NMR powder spectra of PLB at various concentrations incorporated into POPC/POPC- $\text{d}_{31}$  phospholipid bilayers at 35°C. 5.55 mol % POPC- $\text{d}_{31}$  was doped into the POPC sample. The concentration of PLB with respect to POPC is noted on the right side of each spectrum.

earlier. The spectral resolution deteriorates as the concentration of PLB increases, manifested by the disappearance of the sharp edges of the peaks. This suggests intermediate-timescale motions of the lipids induced by the PLB peptide. The changes in the spectral resolution of the  $^2\text{H}$  NMR spectra confirm that PLB interacts with the acyl chains of the lipid bilayers. Interesting features of the  $^2\text{H}$  NMR spectra are the appearance of an isotropic peak in the presence of PLB the intensity of which increases with the amount of PLB. This indicates that the large vesicles are fragmented into smaller size vesicles by increasing the amount of PLB in the POPC bilayers. These results agree with our  $^{31}\text{P}$  NMR data.

Fig. 5 shows the  $^2\text{H}$  NMR spectra of POPC- $\text{d}_{31}$  samples in the presence (4 mol %, dotted line) and in the absence (pure POPC/POPC- $\text{d}_{31}$  bilayers, solid line) of PLB obtained over a temperature ranging from 30°C to 60°C. The shape of the  $^2\text{H}$  NMR spectra of the control POPC/POPC- $\text{d}_{31}$  is a typical  $^2\text{H}$  phospholipid bilayer lineshape ( $L_\alpha$  phase), and looks very similar to those previously reported (Huber et al., 2002; Lafleur et al., 1989; Nezil and Bloom, 1992). As the temperature is raised, the spectra retain their overall lineshape in both cases with and without PLB. The spectral features become narrower due to increased mobility by raising the temperature. The  $^2\text{H}$  NMR spectra with and without 4 mol % PLB did not undergo any substantial changes in the spectral breadth or quadrupolar splitting. Interestingly, the isotropic component observed by the addition of 4 mol % PLB indicates the formation of small

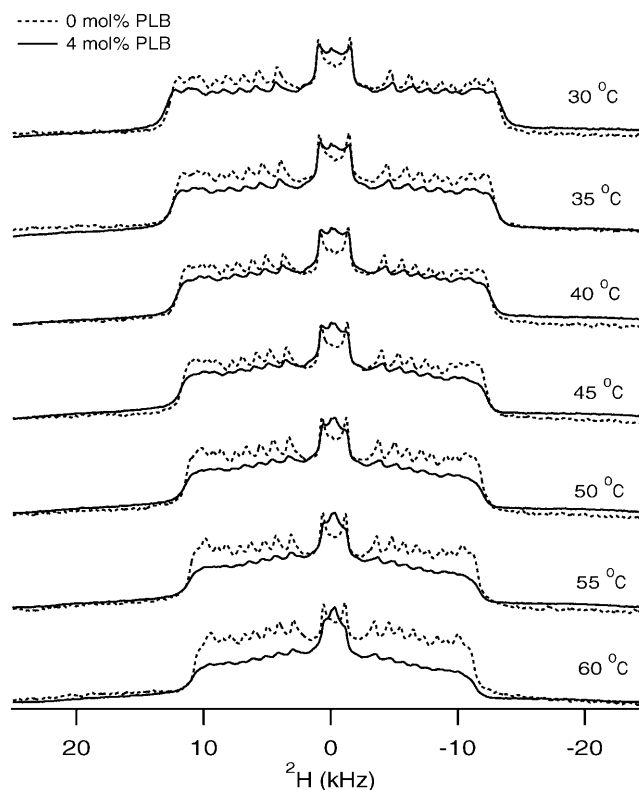


FIGURE 5 Temperature-dependent  $^2\text{H}$  NMR spectra of PLB incorporated into POPC/POPC- $\text{d}_{31}$  phospholipid bilayers. The solid-line spectra represent POPC/POPC- $\text{d}_{31}$  sample prepared in the absence of PLB, whereas the dotted-line spectra represent samples prepared with 4 mol % PLB with respect to POPC. The temperature at which each spectrum was taken is noted on the right side of that spectrum.

vesicles due to the fragmentation of large vesicles throughout the temperature range from 30°C to 60°C. The intensity of the isotropic peak increases as the temperature increases, indicating an increase in the rapid tumbling of small vesicles and/or an increase in lateral diffusion of the phospholipids (Davis, 1979).

The smoothed segmental C-D bond order parameters ( $S_{\text{CD}}$ ) were calculated by dePaking the powder spectra represented in Fig. 5 for the POPC- $\text{d}_{31}$  as a function of temperature (Fig. 6). The  $S_{\text{CD}}$  order parameters depend upon several averaging modes provided by intramolecular, intermolecular, and collective motions (Sanders and Schwoonek, 1992; Seelig and Seelig, 1974; Seelig and Niederberger, 1974). The segmental  $S_{\text{CD}}$  order parameter describes local orientation or dynamic perturbations of the C-D bond vector from its standard state due to perturbations of the POPC phospholipid conformations or dynamics as a result of the addition of PLB. The magnitude of the order parameters ( $S_{\text{CD}} \sim 0.20\text{--}0.30$ ) indicates that the phospholipid bilayers are in the liquid-crystalline phase (Huster et al., 1998; Lafleur et al., 1989). A characteristic profile of decreasing order parameters with increasing distance from the glycerol backbone was obtained both for the pure bilayer and for the

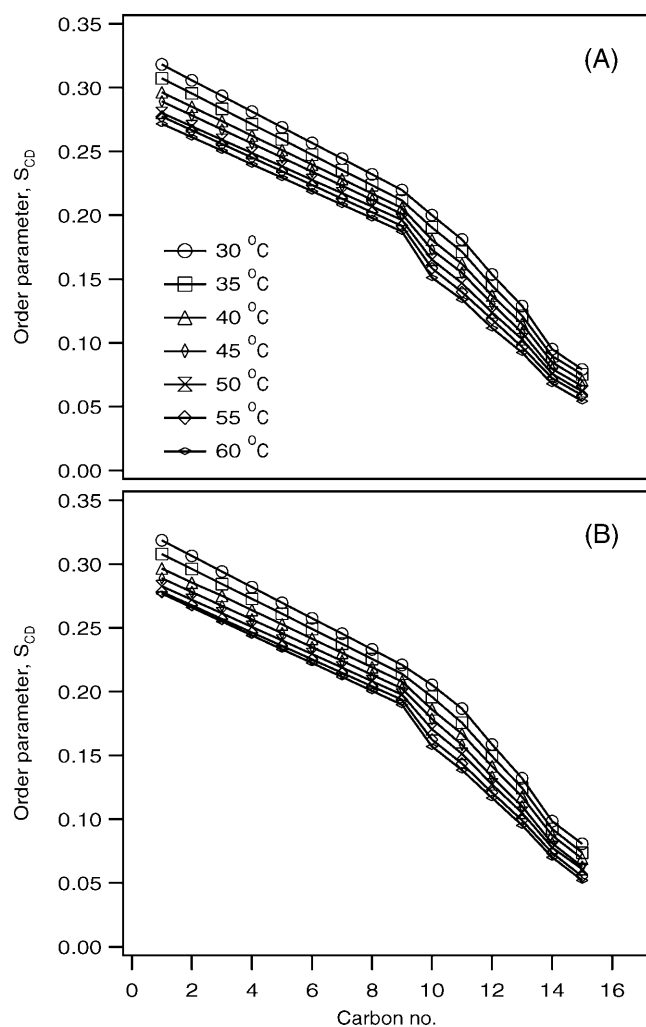


FIGURE 6 Temperature-dependent smoothed acyl chain (POPC- $d_{31}$ ) orientational order  $S_{CD}$  profiles calculated from the dePaked spectra of Fig. 5. (A) Pure POPC bilayer. (B) 4 mol % PLB embedded into the POPC bilayer.

PLB-bound bilayer. These values are comparable with the results previously determined using labeled POPC by NMR, and also recently calculated by using molecular dynamic simulations (Huber et al., 2002; Seelig and Seelig, 1974). The data indicates that there is more disorder and motion in the center and at the end of the acyl chain when compared to the headgroup region in the presence of PLB. Interestingly, the order parameter profile obtained from the sample in the presence of PLB (4 mol %) closely resembles the order parameter profile of pure POPC bilayers. This indicates that the POPC bilayer acyl chains are not significantly perturbed by the addition of PLB at these concentrations. Also, the order parameter profiles indicate (for both cases) that by increasing the temperature, the  $S_{CD}$  values decrease. This is due to a combination of the increase in the mobility of the acyl chains, rapid tumbling of vesicles, and possible increases in lateral diffusion of the POPC phospholipids.

## CONCLUSIONS

In the present study, the  $^{31}\text{P}$  NMR spectra indicated that the hydrophobic segment of phospholamban was incorporated successfully into the fully hydrated dispersed POPC phospholipid bilayers. The spectral simulations of  $^{31}\text{P}$  NMR spectra of samples containing higher concentrations of PLB indicate the presence of different sizes of vesicles. The large phospholipid bilayer vesicles fragmented into smaller vesicles by increasing the concentration of PLB with respect to POPC. Interestingly, the contribution from smaller vesicles increased as the temperature increased. The data indicate that small vesicles are tumbling faster at higher temperatures. Another possibility is that by increasing the amount of PLB incorporated into the POPC bilayer, the lateral diffusion rate of the lipids increases at higher temperatures. In addition to the  $^{31}\text{P}$  NMR studies,  $^2\text{H}$  NMR spectroscopic studies were carried out using POPC- $d_{31}$  to understand the lipid-peptide interactions in the hydrophobic region of the phospholipid bilayers. The data suggest that smaller size vesicles are formed by the addition of 4 mol % PLB into the bilayers and support our  $^{31}\text{P}$  NMR spectral study. The segmental  $S_{CD}$  order parameter indicates that there are no significant changes in the ordering of the acyl chains of the phospholipid bilayers. It suggests that the incorporation of PLB into the POPC bilayers did not significantly perturb the acyl chains of the phospholipid bilayers at these concentrations. In the present paper, solid-state NMR spectroscopic studies were carried out to better understand the lipid-peptide interactions from the membrane perspective utilizing unoriented POPC lipid bilayers. The unoriented phospholipid bilayer samples used in the study with PLB can be used for a variety of magic angle spinning experiments such as REDOR (rotational-echo double-resonance). These experiments can reveal unique structural information on PLB with respect to the membrane. Future solid-state NMR experiments specifically designed to investigate the spatial position and orientation of the PLB with respect to the membrane utilizing site-specific  $^2\text{H}$ -labeled and  $^{15}\text{N}$ -labeled PLB samples mechanically aligned on glass plates are in progress.

This work was supported by an American Heart Association Scientist Development grant (0130396N) and a National Institutes of Health grant (GM60259-01). The 500-MHz wide-bore NMR spectrometer was obtained from a National Science Foundation grant (10116333).

## REFERENCES

- Arora, A., and L. K. Tamm. 2001. Biophysical approaches to membrane protein structure determination. *Curr. Opin. Struct. Biol.* 11:540–547.
- Auger, M. 1997. Membrane structure and dynamics as viewed by solid-state NMR spectroscopy. *Biophys. Chem.* 68:233–241.
- Barre, P., O. Zschoring, K. Arnold, and D. Huster. 2003. Structural and dynamical changes of the bindin B18 peptide upon binding to lipid membranes. *Biochemistry*. 42:8377–8386.



- Bloom, M., E. Evans, and O. G. Mouritsen. 1991. Physical properties of the fluid lipid-bilayer component of cell membrane: a perspective. *Q. Rev. Biophys.* 24:293–397.
- Brunner, E., J. Ogle, M. Wenzler, and H. R. Kalbitzer. 2000. Molecular alignment of proteins in bicellar solutions: Quantitative evaluation of effects induced in 2D COSY spectra. *Biochem. Biophys. Res. Commun.* 272:694–698.
- Burnell, E. E., P. R. Cullis, and B. De Kruijff. 1980. Effects of tumbling and lateral diffusion on phosphatidylcholine model membrane  $^{31}\text{P}$  NMR line shapes. *Biochim. Biophys. Acta.* 1980:63–69.
- Cavagnero, S., H. J. Dyson, and P. E. Wright. 1999. Improved low pH bicelle system for orienting macromolecules over a wide temperature range. *J. Biomol. NMR.* 13:387–391.
- Cross, T. A. 1997. Solid-state nuclear magnetic resonance characterization of gramicidin channel structure. *Methods Enzymol.* 289:672–696.
- Cullis, P. R., and B. de Kruijff. 1979. Lipid polymorphism and the functional roles of lipids in biological membranes. *Biochim. Biophys. Acta.* 559:399–420.
- Dave, P. C., E. K. Tiburu, N. A. Nusair, and G. A. Lorigan. 2003. Calculating order parameter profiles utilizing magnetically aligned phospholipid bilayers for  $^2\text{H}$  NMR studies. *Solid State Nucl. Magn. Reson.* 24:328–339.
- Davis, J. H. 1979. Deuterium magnetic resonance study of the gel and liquid crystalline phases of dipalmitoyl phosphatidylcholine. *Biophys. J.* 27:339–358.
- Davis, J. H., K. R. Jeffrey, M. Bloom, and M. I. Valic. 1976. Quadrupolar echo deuterium magnetic resonance spectroscopy in ordered hydrocarbon chains. *Chem. Phys. Lett.* 42:390–394.
- de Kruijff, B., and P. R. Cullis. 1980. Cytochrome-c specifically induces non-bilayer structures in cardiolipin-containing model membranes. *Biochim. Biophys. Acta.* 902:477–490.
- Dempsey, C. E., N. J. P. Ryba, and A. Watts. 1986. Evidence from deuterium nuclear magnetic resonance for the temperature dependent reversible self association of erythrocyte band-3 in dimyristoylphosphatidylcholine bilayers. *Biochemistry.* 25:2180–2187.
- Dufourc, E. J., E. J. Parish, S. Chitrakorn, and I. C. P. Smith. 1984. Structural and dynamical details of cholesterol-lipid interaction as revealed by deuterium NMR. *Biochemistry.* 23:6062–6071.
- Epand, R. M. 1998. Lipid polymorphism and protein-lipid interactions. *Biochim. Biophys. Acta.* 1376:353–368.
- Fujii, J., A. Ueno, K. Kitano, S. Tanaka, M. Kadoma, and M. Tada. 1987. Characterization of structural unit of phospholamban by amino acid sequencing and electrophoretic analysis. *Biochem. Biophys. Res. Commun.* 138:1044–1050.
- Hallock, K. J., D. K. Lee, and A. Ramamoorthy. 2003. MSI-78, an analogue of the magainin antimicrobial peptides, disrupts lipid structure via positive curvature strain. *Biophys. J.* 84:3052–3060.
- Harzer, U., and B. Bechinger. 2000. Alignment of lysine-anchored membrane peptides under conditions of hydrophobic mismatch: a CD,  $^{15}\text{N}$  and  $^{31}\text{P}$  solid-state NMR spectroscopy investigation. *Biochemistry.* 39:13106–13114.
- Henzler Wildman, K. A., D. K. Lee, and A. Ramamoorthy. 2003. Mechanism of lipid bilayer disruption by the human antimicrobial peptide, LL-37. *Biochemistry.* 42:6545–6558.
- Hori, Y., M. Demura, T. Niidome, H. Aoyagi, and T. Asakura. 1999. Orientational behavior of phospholipid membranes with mastoparan studied by  $^{31}\text{P}$  solid state NMR. *FEBS Lett.* 455:228–232.
- Huber, T., K. Rajamoorthy, V. F. Kurze, K. Bayer, and M. F. Brown. 2002. Structure of docosahexaenoic acid-containing phospholipid bilayers as studied by  $^2\text{H}$  NMR and molecular dynamics simulations. *J. Am. Chem. Soc.* 124:298–309.
- Huster, D., K. Arnold, and K. Garwisch. 1998. Influence of docosahexaenoic acid and cholesterol on lateral lipid organization. *Biochemistry.* 37:17299–17308.
- Huster, D., X. Yao, K. Jakes, and M. Hong. 2002. Conformational changes of colicin Ia channel-forming domain upon membrane binding: a solid-state NMR study. *Biochim. Biophys. Acta.* 1561:159–170.
- Jones, D. T., W. R. Taylor, and J. M. Thornton. 1994. A model recognition approach to the prediction of all-helical membrane protein structure and topology. *Biochemistry.* 33:3038–3049.
- Laflaur, M., B. Fine, E. Stermin, P. R. Cullis, and M. Bloom. 1989. Smoothed orientational order profile of lipid bilayers by  $^2\text{H}$ -nuclear magnetic resonance. *Biophys. J.* 56:1037–1041.
- Lemmon, M. A., and D. M. Engelman. 1994a. Specificity and promiscuity in membrane helix interactions. *FEBS Lett.* 346:17–20.
- Lemmon, M. A., and D. M. Engelman. 1994b. Specificity and promiscuity in membrane helix interactions. *Q. Rev. Biophys.* 27:157–218.
- Liu, F., R. N. A. H. Lewis, R. S. Hodges, and R. N. McElhaney. 2001. A differential scanning calorimetric and  $^{31}\text{P}$  NMR spectroscopic study of the effect of transmembrane  $\alpha$ -helical peptides on the lamellar-reversed hexagonal phase transition of phosphatidylethanolamine model membranes. *Biochemistry.* 40:760–768.
- Long, J. R., J. L. Dindot, H. Zebroski, S. Kihne, R. H. Clark, A. A. Campbell, P. S. Stayton, and G. P. Drobny. 1998. A peptide that inhibits hydroxyapatite growth is in an extended conformation on the crystal surface. *Proc. Natl. Acad. Sci. USA.* 95:12083–12087.
- Long, J. R., W. J. Shaw, P. S. Stayton, and G. P. Drobny. 2001. Structure and dynamics of hydrated statherin on hydroxyapatite as determined by solid-state NMR. *Biochemistry.* 40:15451–15455.
- Marassi, F. M., C. Ma, H. Gratkowski, S. K. Straus, K. Strebel, M. Orblatt-Montal, M. Montal, and S. J. Opella. 1999. Correlation of the structural and functional domains in the membrane protein Vpu from HIV-1. *Proc. Natl. Acad. Sci. USA.* 96:14336–14341.
- Marassi, F. M., and S. J. Opella. 1998. NMR structural studies of membrane proteins. *Curr. Opin. Struct. Biol.* 8:640–648.
- Marcotte, I., E. J. Dufourc, M. Ouellet, and M. Auger. 2003. Interaction of the neuropeptide Met-Enkephalin with zwitterionic and negatively charged bicelles as viewed by  $^{31}\text{P}$  and  $^2\text{H}$  solid-state NMR. *Biophys. J.* 85:328–339.
- Mascioni, A., C. Karim, J. Zamoan, D. D. Thomas, and G. Vegila. 2002a. Solid-state NMR and rigid body molecular dynamics to determine domain orientations of monomeric phospholamban. *J. Am. Chem. Soc.* 124:9392–9393.
- Mascioni, A., C. Karim, G. Barany, D. D. Thomas, and G. Vegila. 2002b. Structure and orientation of sacrolopin in lipid environments. *Biochemistry.* 41:475–482.
- Massiot, D., F. Fayon, M. Capron, I. King, S. Le Calve, B. Alonso, J. O. Durand, B. Bujoli, Z. Gan, and G. Hoatson. 2002. Modelling one- and two-dimensional solid-state NMR spectra. *Magn. Reson. Chem.* 40:70–76.
- McCabe, M. A., and S. R. Wassall. 1995. Fast-Fourier-transform dePacking. *J. Magn. Reson. B.* 106:80–82.
- McCabe, M. A., and S. R. Wassall. 1997. Rapid deconvolution of NMR powder spectra by weighted fast Fourier transformation. *Solid State Nucl. Magn. Reson.* 10:53–61.
- Morrow, M. R., and C. W. M. Grant. 2000. The EGF-receptor transmembrane domain: peptide-peptide interactions in fluid bilayer membranes. *Biophys. J.* 79:2024–2032.
- Nakazawa, Y., and T. Asakura. 2003. Structure determination of a peptide model of the repeated helical domain in Samia cynthia ricini silk fibroin before spinning by a combination of advanced solid-state NMR methods. *J. Am. Chem. Soc.* 125:7230–7237.
- Nezil, F. A., and M. Bloom. 1992. Combined influence of cholesterol and synthetic amphiphilic peptides upon bilayer thickness in model membranes. *Biophys. J.* 61:1176–1183.
- Nicholson, L. K., and T. A. Cross. 1989. Gramicidin cation channel: an experimental determination of the right-handed helix sense and verification of beta-type hydrogen bonding. *Biochemistry.* 28:9379–9385.

- Ottiger, M., and A. Bax. 1999. Bicelle-based liquid crystals for NMR-measurement of dipolar couplings at acidic and basic pH values. *J. Biomol. NMR*. 13:187–191.
- Pinheiro, T. J. T., M. J. Duer, and A. Watts. 1997. Phospholipid headgroup dynamics in DOPC- $d_5$ -cytochrome c complexes as revealed by  $^2\text{H}$  and  $^{31}\text{P}$  NMR: the effects of a peripheral protein on collective lipid fluctuations. *Solid State Nucl. Magn. Reson.* 8:55–64.
- Pinheiro, T. J. T., and A. Watts. 1994a. Lipid specificity in the interaction of cytochrome-c with anionic phospholipid-bilayers revealed by solid-state P-31 NMR. *Biochemistry*. 33:2451–2458.
- Pinheiro, T. J. T., and A. Watts. 1994b. Resolution of individual lipids in mixed phospholipid membranes and specific lipid-cytochrome c interactions by magic-angle spinning solid-state P-31 NMR. *Biochemistry*. 33:2459–2467.
- Rigby, A. C., K. R. Barber, G. S. Shaw, and C. W. M. Grant. 1996. Transmembrane region of the epidermal growth factor receptor: behavior and interactions via  $^2\text{H}$  NMR. *Biochemistry*. 35:12591–12601.
- Sanders, C. R., and J. P. Schwonek. 1992. Characterization of magnetically orientable bilayers in mixtures of dihexanoylphosphatidylcholine and dimyristoylphosphatidylcholine by solid-state NMR. *Biochemistry*. 31:8898–8905.
- Seelig, J. 1978.  $^{31}\text{P}$  Nuclear magnetic resonance and the head group structure of phospholipids in membranes. *Biochim. Biophys. Acta*. 515:105–140.
- Seelig, J., and W. Niederberger. 1974. Deuterium-labeled lipids as structural probes in liquid crystalline bilayers. A deuterium magnetic resonance. *J. Am. Chem. Soc.* 96:2069–2072.
- Seelig, A., and J. Seelig. 1974. The dynamic structure of fatty acyl chains in a phosphatidylcholine bilayer measured by deuterium magnetic resonance. *Biochemistry*. 13:4839–4845.
- Sharpe, S., K. R. Barber, C. W. M. Grant, D. Goodyear, and M. R. Morrow. 2002a. Organization of model helical peptides in lipid bilayers: insight into the behavior of single-span protein transmembrane domains. *Biophys. J.* 83:345–358.
- Sharpe, S., K. R. Barber, C. W. M. Grant, and M. R. Morrow. 2002b. Evidence of a tendency to self-association of the transmembrane domain of ErbB-2 in fluid phospholipid bilayers. *Biochemistry*. 41:2341–2352.
- Shaw, W. J., J. R. Long, J. L. Dindot, A. A. Campbell, P. S. Stayton, and G. P. Drobny. 2000. Determination of statherin N-terminal peptide conformation on hydroxyapatite crystals. *J. Am. Chem. Soc.* 122:1709–1716.
- Simmerman, H. K. B., J. H. Collins, J. L. Theibert, A. D. Wegner, and L. R. Jones. 1986. Sequence analysis of phospholamban: identification of phosphorylation sites and two major structural domains. *J. Biol. Chem.* 261:13333–13341.
- Simmerman, H. K. B., and L. R. Jones. 1998. Phospholamban: protein structure, mechanism of action, and role in cardiac function. *Physiol. Rev.* 78:921–947.
- Simmerman, H. K. B., Y. M. Kobayashi, J. M. Autry, and L. R. Jones. 1996. A leucine zipper stabilizes the pentameric membrane domain of phospholamban and forms a coiled-coil pore structure. *J. Biol. Chem.* 271:5941–5946.
- Singer, S. L., and G. L. Nicolson. 1972. The fluid mosaic model of the structure of cell membranes. *Science*. 175:720–731.
- Smith, I. C. P., and I. H. Ekiel. 1984. Phosphorus-31 NMR of phospholipids in membranes, Chapter 5. In *Phosphorus-31 NMR*. D. G. Gorenstein, editor. Academic Press, New York. 447–475.
- Stockson, G. W., C. F. Polnaszek, A. P. Tulloch, F. Hasan, and I. C. P. Hasan. 1976. Molecular motion and order in single bilayer vesicles and multilamellar dispersions of egg lecithin and lecithin-cholesterol mixtures. A deuterium nuclear magnetic resonance study of specifically labeled lipids. *Biochemistry*. 15:954–966.
- Stokes, D. L. 1997. Keeping calcium in its place:  $\text{Ca}^{2+}$ -ATPase and phospholamban. *Curr. Opin. Struct. Biol.* 7:550–558.
- Strandberg, E., T. Sparrman, and G. Lindblom. 2001. Phase diagrams of systems with cationic  $\alpha$ -helical membrane-spanning model peptides and dioleoylphosphatidylcholine. *Adv. Colloid Interface Sci.* 89–90:239–261.
- Tiburu, E. K., P. C. Dave, J. F. Vanlerberghe, T. B. Cardon, R. E. Minto, and G. A. Lorigan. 2003. An improved synthetic and purification procedure for the hydrophobic segment of the transmembrane peptide phospholamban. *Anal. Biochem.* 318:146–151.
- Vold, R. R., R. S. Prosser, and A. J. Deese. 1997. Isotropic solutions of phospholipid bicelles: a new membrane mimetic for high-resolution NMR studies of polypeptides. *J. Biomol. NMR*. 9:329–335.
- Watts, A. 1981. Protein-lipid interactions: do the spectroscopists now agree? *Nature*. 294:512–513.
- Watts, A. 1993. Magnetic resonance studies of phospholipid-protein interactions in bilayers. In *Phospholipids Handbook*. G. Cevc, editor. Marcel Dekker, New York. 687–744.
- Watts, A. 1998. Solid-state NMR approaches for studying the interaction of peptides and proteins with membranes. *Biochim. Biophys. Acta*. 1376:297–318.
- Yao, Q., L. T. L. Chen, J. Li, K. Brungardt, T. C. Squier, and D. J. Bigelow. 2001. Oligomeric interactions between phospholamban molecules regulate  $\text{Ca}$ -ATPase activity in functionally reconstituted membranes. *Biochemistry*. 40:6406–6413.
- Ying, W., S. E. Irvine, R. A. Beekman, D. J. Siminovitch, and S. O. Smith. 2000. Deuterium NMR reveals helix packing interactions in phospholamban. *J. Am. Chem. Soc.* 122:11125–11128.